Optimization of enhanced terahertz transmission through arrays of subwavelength apertures

C. Janke, J. Gómez Rivas, C. Schotsch, L. Beckmann, P. Haring Bolivar, and H. Kurz
Institut für Halbleitertechnik, RWTH Aachen, D-52056 Aachen, Germany

(Received 20 February 2004; revised manuscript received 23 March 2004; published 21 May 2004)

A detailed study of enhanced transmission of terahertz (THz) radiation through arrays of subwavelength apertures structured in *n*-type silicon is presented. The enhancement is attributed to the resonant tunneling of surface-plasmon polaritons (SPP's) that can be excited at THz wavelengths in doped semiconductors. We investigate the dependence of the transmission as a function of aperture size and sample thickness. The transmission increases significantly as the aperture size is augmented and as the array thickness is reduced. The data confirm the tunneling character of the SPP phenomenon. Transmission efficiencies larger than unity for aperture sizes well below the cutoff wavelength are achieved.

DOI: 10.1103/PhysRevB.69.205314 PACS number(s): 73.20.Mf, 42.79.Dj, 72.80.Cw

I. INTRODUCTION

The discovery of enhanced transmission of light through thin metal gratings of sub-wavelength holes by Ebbesen *et al.*[1] sparked renewed and strongly growing interest in the underlying science and possible applications of surface-plasmon related phenomena.[2–5] The optical transmission at wavelengths above the cutoff defined by the aperture size can be enhanced by several orders of magnitude leading to the extraordinary result of transmission efficiencies larger than 1 (when normalized to the relative area of the apertures).[6,7] This enhanced transmission is successfully explained in terms of resonant tunneling of surface-plasmon polaritons (SPP's).[8–11] Incident light can excite SPP's on the metal due to the periodic structure whereby radiation is collected from an area larger than the aperture. The SPP's tunnel through the aperture and are recoupled into free-space radiation at the opposite interface. As shown by Lezec *et al.*,[12] it is also possible to enhance and collimate the transmission through a single aperture of subwavelength dimensions in a metallic film. To obtain this enhancement and collimation effect, it is required that both sides of the film are periodically structured.[13,14] This extraordinary transmission of light through subwavelength apertures is expected to find numerous applications in fields such as near-field microscopy, photolithography, high-density optical data storage, and optical displays.

The large permittivity of metals at lower than optical frequencies was believed to be a limitation for the scalability of the enhanced transmission phenomenon. However, as pointed out in Ref. 13, the corrugation of the surface gives rise to an effective impedance or permittivity for surface modes. This favors the establishment of SPP's and enables enhanced transmission through metal gratings across an extended part of the electromagnetic spectrum. Furthermore, the scalability to lower frequencies is favored by use of semiconductors instead of metals. Doped semiconductors show metallic behavior at terahertz (THz) frequencies with permittivities similar to those of metals at optical frequencies and therefore allow the excitation of SPP's in this frequency range.

Recently, enhanced transmission of THz radiation through arrays of subwavelength apertures was demonstrated by use of silicon gratings.[15] The transmission was investigated as a function of the grating's lattice constant and a significant enhancement for wavelengths up to seven times larger than the aperture size was reported. This unprecedented transmission enhancement sets the basis for the development of new devices such as, e.g., high-throughput and high spatial resolution filters and focusing elements for THz imaging systems. Moreover, the approach of using semiconductor gratings opens the way to tunable devices. The tuning can be achieved by controlling parameters such as the carrier density which directly influences the generation and propagation of SPP's via the material's dielectric function.

In this paper, we investigate two different routes to optimize the transmission through arrays of subwavelength apertures manufactured from *n*-doped silicon. In particular, we study the transmission through arrays with varying aperture size and grating thickness while the lattice constant remains fixed. The size of the largest aperture is chosen such that the major part of the wavelength spectrum used in the measurements is well above the cutoff wavelength. The thicknesses are chosen to ensure that unstructured samples are opaque to the incident radiation, i.e., no radiation is transmitted directly through the grating material.

II. TERAHERTZ TIME-DOMAIN SPECTROSCOPY

The transmission measurements presented here are carried out with a THz time-domain spectroscopy setup. A pulse train derived from a mode-locked Ti:sapphire femtosecond laser is split into excitation (pump) and detection (probe) pulses. The excitation pulses impinge on an InGaAs surface field emitter which leads to the emission of coherent, pulsed THz radiation via acceleration of photogenerated electron-hole pairs in the semiconductor surface field.[16] The radiation emitted into the specular reflection direction is collected and focused onto the sample with a pair of off-axis parabolic mirrors. Another pair of parabolic mirrors guides the transmitted radiation onto a photoconductive antenna which is gated by the probe pulses. This enables the time domain detection of the coherent THz field amplitude by scanning the time delay between pump and probe pulses with a motorized translation stage. By detecting the electromagnetic field amplitude rather than the time averaged intensity, the

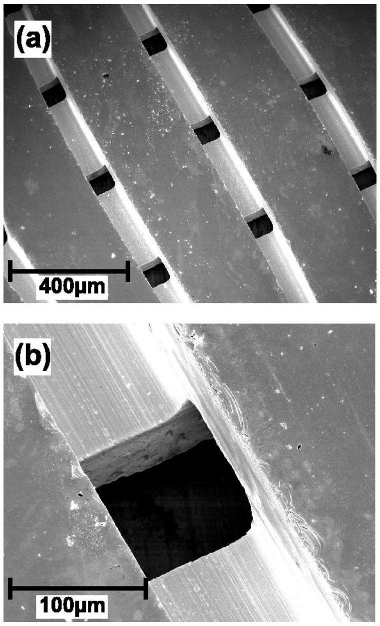

FIG. 1. (a) SEM micrograph of a square grating with subwavelength holes as manufactured by the procedure outlined in the text. The size of the apertures and the lattice constant are determined by the width and the spacing of the cuts, respectively. (b) Magnification showing a single aperture.

complex Fourier transform of the time-domain data directly provides the amplitude and phase spectrum of the broadband THz pulse. A comparison of the obtained frequency spectra with and without a sample in the beam path thus allows the determination of the sample's spectral transmission properties. The usable spectral range of the setup extends from 2.5 to about 0.4 THz or 120 to 700 μm, respectively. The spectral resolution is 20 GHz (as determined by the temporal scanning length of 50 ps) which relates to approximately 6 μm in terms of wavelength.

III. SAMPLE FABRICATION

For the fabrication of the gratings a 3 in. *n*-doped silicon wafer with an initial thickness of 270 μm and a carrier concentration of $N \simeq 10^{18}$ cm^{-3} is used. As a first step in the preparation process the wafer is cut into square pieces of 15×15 mm^2 with a dicing saw (Disco DAD 321). The thickness d of these pieces is reduced to 100 μm$\leqslant d \leqslant 270$ μm with a tolerance of about ± 5 μm. Samples thinner than 100 μm are not mechanically stable enough to be further processed. After reducing the thickness, the apertures are fabricated by use of the dicing saw again: parallel cuts with separation a_0 and depth $d/2$ are made on one side, the sample is then turned over and rotated by 90°, and perpendicular cuts are made on the reverse side. This procedure leads to an array of square apertures with lattice constant a_0. The size of the apertures is determined by the width of the cutting blade, w, ranging from $w = 45$ to 130 μm. The lattice constant of all samples in this study is kept constant at $a_0 = 400$ μm. In Fig. 1(a), a scanning electron microscope picture of a grating structure with $a_0 = 400$ μm and $w = 110$ μm is shown. A higher magnification image of one of the apertures is shown in Fig. 1(b).

IV. RESONANT TUNNELING OF SPP'S

The transmission through the samples is measured at normal incidence of the THz radiation. In this configuration and for a square lattice, the resonant wavelengths for the excitation of SPP's are approximately given by[6,17]

$$\lambda_{\text{SPP}}^{l,m} \simeq \frac{a_0}{\sqrt{l^2+m^2}} \sqrt{\frac{\epsilon_1 \epsilon_2}{\epsilon_1 + \epsilon_2}}, \tag{1}$$

where a_0 is the lattice constant, ϵ_1 is the permittivity of the grating material, ϵ_2 is the permittivity of the dielectric surrounding the grating, and l,m are integer mode indices. Due to the square symmetry of the gratings the resonances are twofold degenerate, i.e., $\lambda^{l,m} = \lambda^{m,l}$.

The periodic surface corrugation also leads to the generation of modes diffracted into the plane of the grating surface. This gives rise to the formation of pronounced minima in the transmission spectra which are known as Wood's anomaly.[18] For normal incidence and a square lattice the corresponding wavelengths are approximately given by[19]

$$\lambda_{\text{Wood}}^{l,m} \simeq \frac{a_0}{\sqrt{l^2+m^2}} \sqrt{\epsilon_2}. \tag{2}$$

Because the samples are fabricated from *n*-doped silicon with a carrier concentration of $N \simeq 10^{18}$ cm^{-3}—leading to a permittivity of $\epsilon_1 \simeq -18$ at 1 THz in a straightforward Drude-type calculation—and the surrounding dielectric is air (i.e., $\epsilon_2 \simeq 1$), the SPP wavelengths given by Eq. (1) will differ only slightly from the wavelengths at which Wood's anomaly occurs. It is thus likely that the minima of Wood's anomaly partially overlap with the SPP resonances.

Specific investigations of the role of the permittivities ϵ_1 and ϵ_2 in the optical wavelength regime can be found in Refs. 19–21. As mentioned above, the lattice constant a_0 can be varied by changing the spacing between consecutive cuts. A detailed study of the dependence of the resonant wavelength on the *lattice constant* in the THz frequency range is presented in Ref. 15. In the following we focus on the dependence of the resonant transmission characteristics on the *size* of the subwavelength apertures and on the *thickness* of the grating structures.

A. Dependence of the transmission on the aperture size

To determine the transmission dependence on the aperture size four different gratings with apertures of side length $w = 45$, 70, 110, and 130 μm, fixed thickness $d = 100$ μm, and lattice constant $a_0 = 400$ μm were used. Figure 2 shows the measured transmission spectra as function of wavelength from 120 to 700 μm, or, in terms of frequency from 2.5 to about 0.4 THz. The spectra are normalized with respect to a reference measurement (cf. Sec. II).

The data show the overall increase of the relative transmission as the aperture size is increased from 45 to 130 μm.

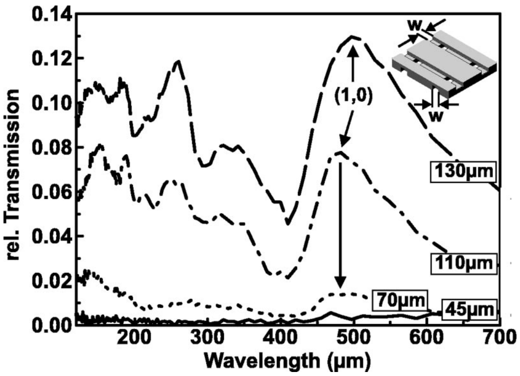

FIG. 2. Transmission spectra as function of wavelength for apertures with $w=45$, 70, 110, and 130 μm. The thickness is $d=100$ μm for all samples. The numbers in brackets denote the SPP mode indices.

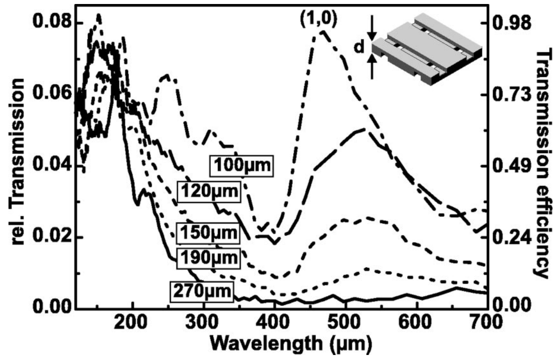

FIG. 3. Transmission spectra as function of wavelength for different grating thicknesses $d=270$, 190, 150, 120, and 100 μm and aperture size $w=110$ μm.

For an aperture size of 130 μm (dashed line in Fig. 2) and 110 μm (dash-dotted line) a pronounced peak at a wavelength of about 500 μm is obtained. This peak can be assigned to the (1,0)-SPP resonance and is labeled accordingly with the respective mode indices (l,m). Higher-order resonances also seem to appear at shorter wavelengths but fall within the half-wavelength cutoff range for the respective aperture sizes. For an aperture size of 70 μm this behavior is strongly attenuated while for 45 μm hardly any spectral features are visible.

At wavelengths of approximately 400, 280, 230, 200, and 180 μm minima occur in the spectra in agreement with Eq. (2) for Wood's anomaly. In contrast, the (1,0)-SPP peak occurs at a wavelength much longer than to be expected from Eq. (1). Also, the position of the largest (1,0) peak (dashed line in Fig. 2) appears to be shifted towards longer wavelengths with respect to the other peaks, as indicated by the slanted arrow. This shift may be attributed to two effects: The first one being merely a side effect of Wood's anomaly which truncates the SPP resonance whereby a feigned shift is produced. The second one is the dependence of the SPP dispersion relation on the surface corrugation. This dependence is discussed in Ref. 11 and a similar shift is predicted for an array of subwavelength holes in a silver film at optical wavelengths.

The spectral shift of the resonances as whole can be ascribed to the following reasons: The expression for the resonance wavelength for square arrays of subwavelength holes as given by Eq. (1) is of approximative nature.[6] Although our samples form square arrays of subwavelength apertures, the apertures themselves are opened by perpendicular cuts on the top and bottom side of the sample. This leads to half-open apertures (see Fig. 1) rather than actual holes as obtained, e.g., by drilling. Thus, the applicability of Eq. (1) to our structure is limited and a more refined theory is needed. Another possibility for the spectral shift is, as outlined before, interference with Wood's anomalies.

Nonetheless, the exceptional, above cutoff transmittance is clearly evident. The (1,0) resonance for an aperture size of $w=130$ μm peaks at a relative transmission of about 13%. Since in this case the area taken up by apertures with respect to the otherwise opaque sample is only 12%, the actual transmission efficiency is 110%. Thus, more radiation is transmitted through an aperture than actually impinges onto it. Similarly, for an aperture size of $w=110$ μm the transmission efficiency is found to be 100%. For $w=70$ μm the efficiency is roughly 45%. Even though less dramatic than for the larger apertures this value still signifies enhancement. Standard theory for a single subwavelength aperture predicts transmission efficiencies of the order of only 1%. The greater than unity transmittance for the largest aperture is in agreement with values reported in the optical wavelength regime for a square array with subwavelength holes.[11] However, Thio *et al.*[7] found the normalized transmittance in a square lattice to depend on the lattice constant only and not on the size of the apertures. This discrepancy might again be due to the aforementioned difference between the type of apertures and holes used in the respective investigations.

B. Dependence of the transmission on the grating thickness

The dependence of the spectral transmission characteristics on the grating thickness d is investigated with five samples with $d=270$, 190, 150, 120, and 100 μm. All samples have the same aperture size ($w=110$ μm) and lattice constant ($a_0=400$ μm). The normalized transmission spectra are shown as function of wavelength in Fig. 3. The vertical scale on the right-hand side shows the actual transmission efficiency which is obtained by relating the measured relative transmission to the fraction of the sample area occupied by apertures. (cf. Sec. IV A).

The overall transmission increases as the grating thickness is reduced from $d=270$ to 100 μm. The first SPP resonance is obtained for $d=100$, 120, 150, and 190 μm at a wavelength of about 500 μm. The thickest grating ($d=270$ μm, solid line) does not show any spectral features at this wavelength within the detection limit of our experiment. Again, Wood's anomalies are present at 400 μm and 200 μm. The general increase of the transmission occurring for all samples below a wavelength of 220 μm is a manifestation of the cutoff wavelength determined by the 110 μm-aperture size.

Again, the transmission enhancement is clearly visible with transmission efficiencies ranging from 17% for d

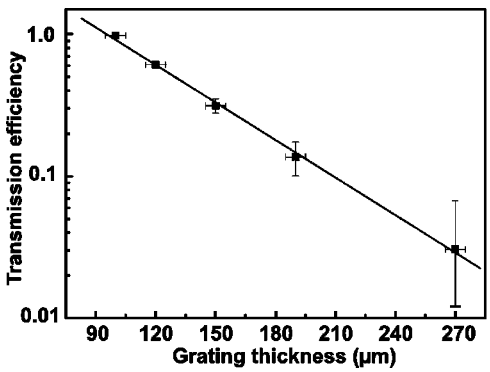

FIG. 4. Amplitude of the (1,0)-resonance peak as function of grating thickness on a logarithmic scale. The horizontal error bars correspond to the variation in thickness of about ± 5 μm, the vertical error bars reflect the noise level of the measurement.

$=190$ μm to almost 100% for $d=100$ μm. Most remarkably, the transmission at the SPP resonance wavelength ($\lambda_{\rm SPP}^{1,0} \simeq 500$ μm) for the thinnest grating is almost the same as for wavelengths well below the cutoff. In Fig. 4 the peak amplitude of the (1,0) resonance is plotted as function of grating thickness on a logarithmic scale. The dependence is found to be rigorously exponential in close resemblance to experimental observations and theoretical studies at optical wavelengths (Ref. 22 and Ref. 11, respectively). The characteristic decay length extracted from a fit to the data is $L_{\rm exp} = 44(\pm 1)$ μm. The exponential decay reflects the evanescent, i.e., nonpropagating nature of the SPP mode.

For comparison, a rectangular waveguide in a perfect conductor can be assumed as a simplistic model for our structure. Classical waveguide theory predicts a decay length of[23]

$$L_{\rm theor} = \frac{\lambda_0}{2\pi} \frac{1}{\sqrt{\left(\frac{\lambda_0}{2w}\right)^2 - 1}} \tag{3}$$

for wavelengths above cutoff, i.e., in a regime where no propagating modes are supported. λ_0 is the wavelength in the unbounded medium and w is the size of the aperture. With $\lambda_0 = \lambda_{\rm SPP}^{1,0} \simeq 500$ μm and $w = 110$ μm a value of $L_{\rm theor} \simeq 39$ μm is obtained from Eq. (3) which matches the experimental value derived from our measurements fairly well. This once more underpins the nonpropagating behavior inside the apertures and thus the tunneling mechanism of the SPP-enhanced transmission.

V. CONCLUSION

The extraordinary transmission of radiation through arrays of subwavelength apertures was investigated at THz frequencies. These arrays can be easily manufactured from highly doped silicon wafers with a dicing saw. We studied the characteristic transmission behavior by systematically varying the aperture size and thickness of the grating structures. The observed maxima and minima in the measured transmission spectra are attributed to resonant tunneling of SPP's and Wood's anomalies, respectively. Transmission efficiencies exceeding unity for wavelengths well above cutoff are found for certain aperture sizes and grating thicknesses whereby a guiding principle for future structure design is provided. Our measurements generally confirm results obtained at optical frequencies and thus prove the generality of the extraordinary transmission effect based on resonant tunneling of SPP's. Consequently, with the right choice of materials and dimensions, no principal limitation for other wavelength regimes should be encountered. The unique transmission properties observed here are foreseen to be exploited for, e.g., novel high-throughput and high spatial resolution and focusing devices for THz imaging systems.

ACKNOWLEDGMENTS

We gratefully acknowledge valuable discussions with F. J. García-Vidal and L. Martín-Moreno and financial support from the European Union through the TMR project *Interaction*.

[1] T. Ebbesen, H. Lezec, H. Ghaemi, T. Thio, and P. Wolff, Nature (London) **391**, 667 (1998).
[2] W. Barnes, A. Dereux, and T. Ebbesen, Nature (London) **424**, 824 (2003).
[3] S. Seidel, S. Grafström, L. Eng, and L. Bischoff, Appl. Phys. Lett. **82**, 1368 (2003).
[4] E. Altewischer, M. van Exter, and J. Woerdmann, Nature (London) **418**, 304 (2002).
[5] S. Shinada, J. Hashizume, and F. Koyama, Appl. Phys. Lett. **83**, 836 (2003).
[6] H. Ghaemi, T. Thio, D. Grupp, T. Ebbesen, and H. Lezec, Phys. Rev. B **58**, 6779 (1998).
[7] T. Thio, H. Ghaemi, H. Lezec, P. Wolff, and T. Ebbesen, J. Opt. Soc. Am. B **16**, 1743 (1999).
[8] U. Schröter and D. Heitmann, Phys. Rev. B **58**, 15 419 (1998).
[9] W. Tan, T. Preist, and R. Sambles, Phys. Rev. B **62**, 11 134 (2000).
[10] E. Popov, M. Nevière, S. Enoch, and R. Reinisch, Phys. Rev. B **62**, 16 100 (2000).
[11] L. Martín-Moreno, F. García-Vidal, H. Lezec, K. Pellerin, T. Thio, J. Pendry, and T. Ebbesen, Phys. Rev. Lett. **86**, 1114 (2001).
[12] H. Lezec, A. Degiron, E. Devaux, R. Linke, L. Martín-Moreno, F. García-Vidal, and T. Ebbesen, Science **297**, 820 (2002).
[13] L. Martín-Moreno, F. García-Vidal, H. Lezec, A. Degiron, and T. Ebbesen, Phys. Rev. Lett. **90**, 167401 (2003).
[14] F. García-Vidal, L. Martín-Moreno, H. Lezec, and T. Ebbesen, Appl. Phys. Lett. **83**, 4500 (2003).
[15] J. Gómez Rivas, C. Schotsch, P. Haring Bolivar, and H. Kurz, Phys. Rev. B **68**, 201306 (2003).
[16] X.-C. Zhang and D. Auston, J. Appl. Phys. **71**, 326 (1992).
[17] H. Raether, *Surface Plasmons on Smooth and Rough Surfaces and on Gratings* (Springer-Verlag, Berlin, 1988).
[18] R. Wood, Phys. Rev. **48**, 928 (1935).

[19] T. Kim, T. Thio, T. Ebbesen, D. Grupp, and H. Lezec, Opt. Lett. **24**, 256 (1999).
[20] D. Grupp, H. Lezec, T. Ebbesen, K. Pellerin, and T. Thio, Appl. Phys. Lett. **77**, 1569 (2000).
[21] A. Krishnan, T. Thio, T. Kim, H. Lezec, T. Ebbesen, P. Wolff, J. Pendry, L. Martín-Moreno, and F. García-Vidal, Opt. Commun. **200**, 1 (2001).
[22] A. Degiron, H. Lezec, W. Barnes, and T. Ebbesen, Appl. Phys. Lett. **81**, 4327 (2002).
[23] J. Kraus and K. Carver, *Electromagnetics* (McGraw-Hill, New York, 1973).